Supporting Information

Nanocrystalline Ag_3PO_4 for sunlight and ambient air driven oxidation of amines: high photocatalytic efficiency and a facile catalyst regeneration strategy

Reeya Garg,[1,#] Sanjit Mondal,[1,#] Lipipuspa Sahoo,[1] C. P. Vinod,[2] Ujjal K. Gautam[*1]

[1]Department of Chemical Sciences, Indian Institute of Science Education and Research (IISER)-Mohali, Sector 81, Mohali, SAS Nagar, Punjab 140306, India

[2]Catalysis and Inorganic Chemistry Division, CSIR-NCL, Pune 411008, India

[#] These authors contributed equally to this work

*Corresponding author:*ujjalgautam@iisermohali.ac.in*

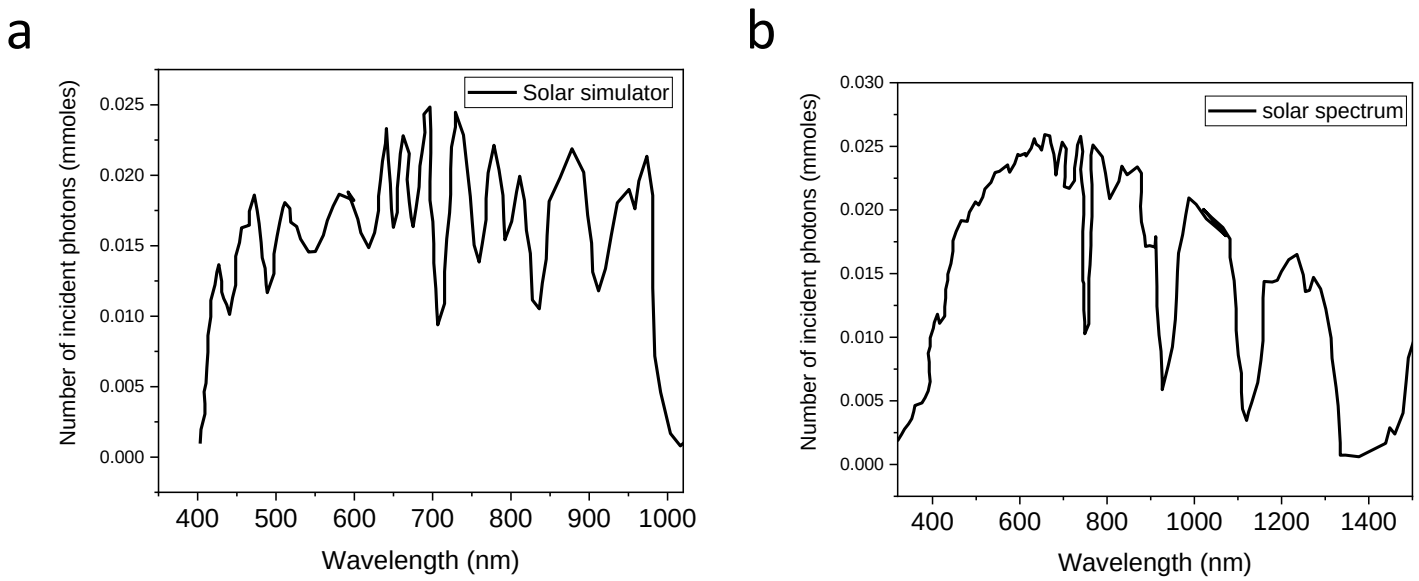

Figure S1. Spectra of the solar simulator (a) and sunlight at sea level (b).

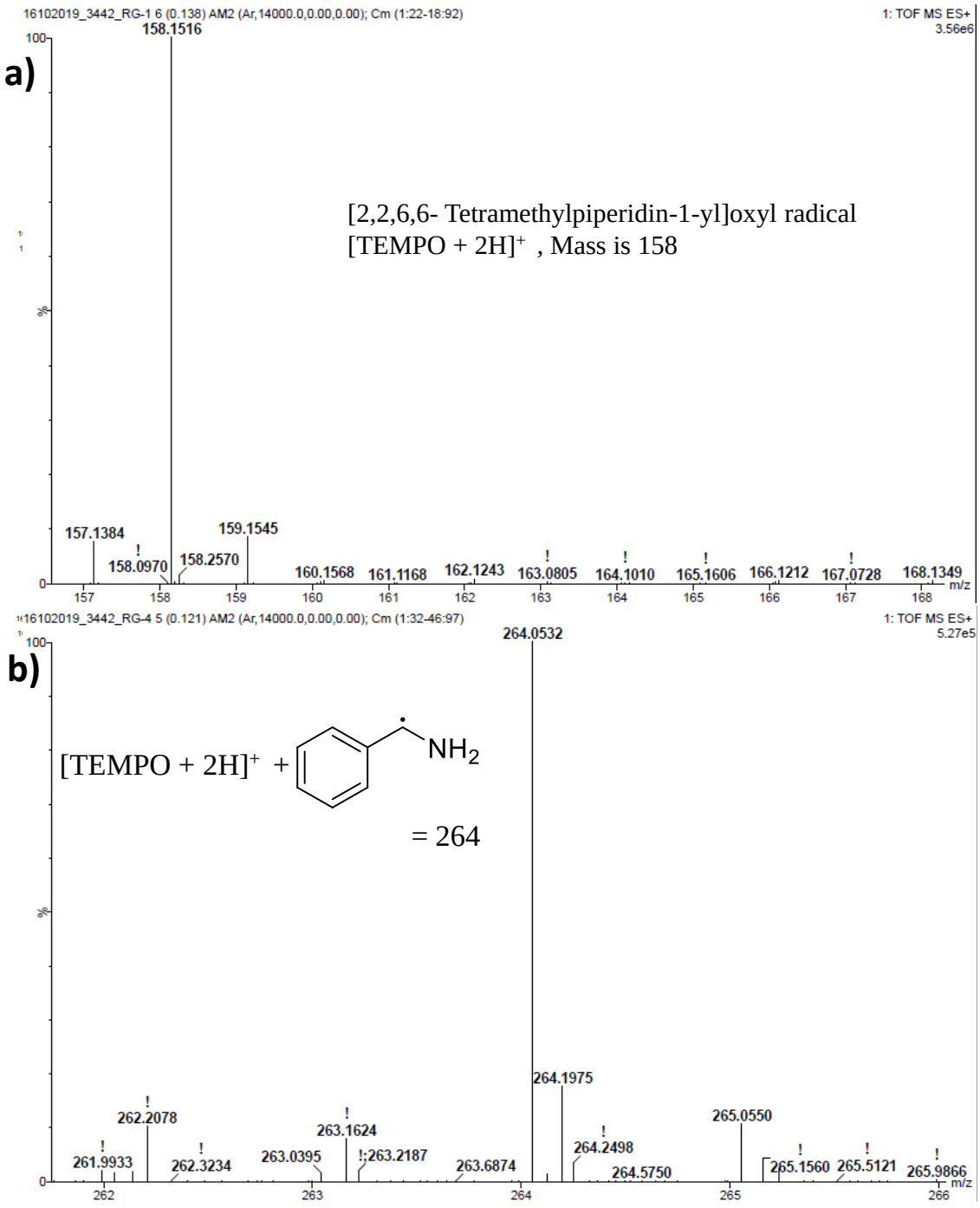

Figure S2. TEMPO was added into oxidation reaction mixture of benzylamine by Ag_3PO_4. HRMS spectra were recorded before start of experiment and after irradiation with light for 20 min. At the start of the reaction, TEMPO + acetonitrile gives $[TEMPO + 2H]^+$ (a) and after irradiation with light, TEMPO forms an adduct with carbon radical species photogenerated from benzylamine (b).[1]

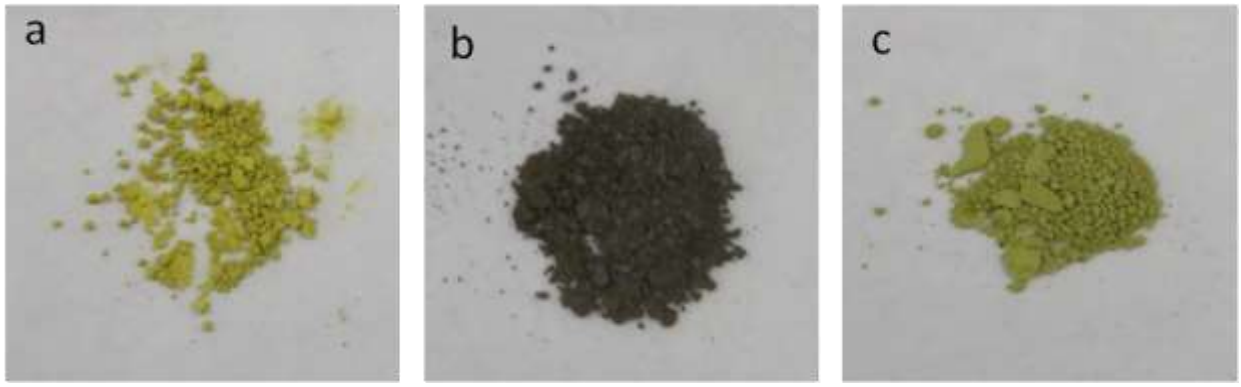

Figure S3. Photographs of Ag_3PO_4: as-synthesized (a), after catalysis (b) and after regeneration (c).

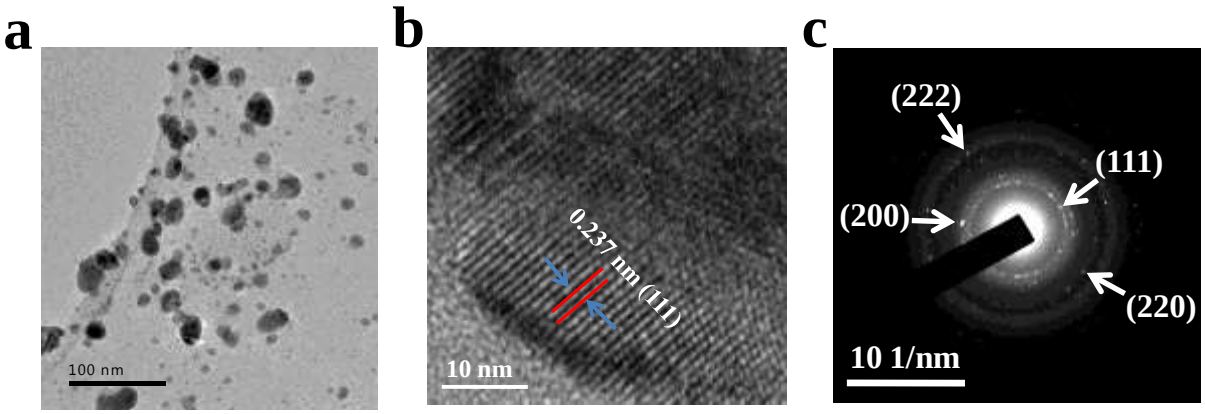

Figure S4. TEM image (a), HR-TEM image (b) and SAED (c) of the Ag_3PO_4 after catalysis confirming the formation of Ag nanoparticles during the photocatalytic reaction. The planes indexed in the SAED pattern corresponds to the FCC phase of Ag.

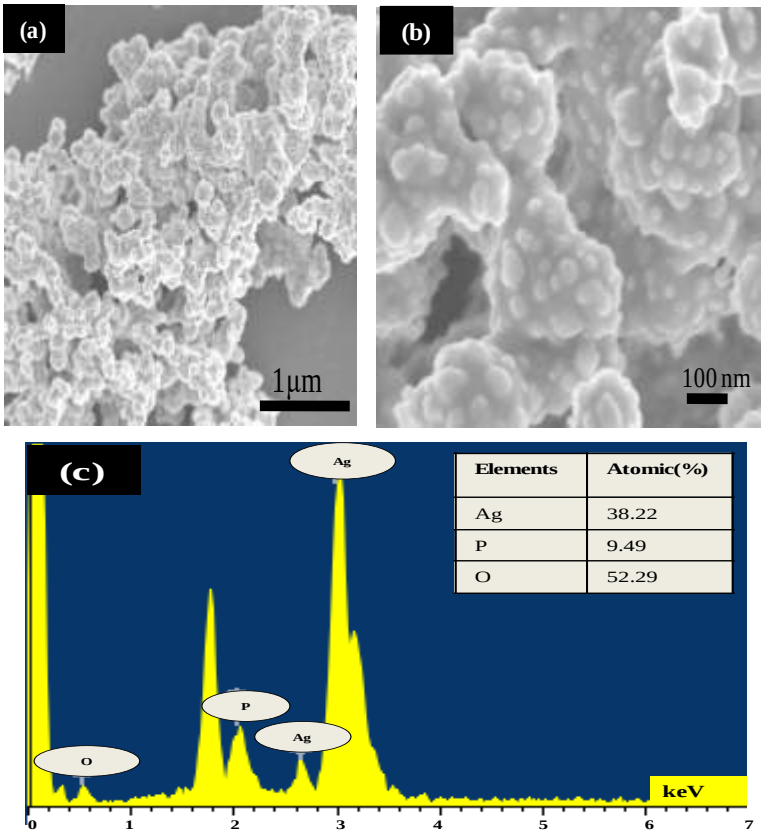

Figure S5. SEM images of regenerated Ag_3PO_4 after catalysis (a, b). SEM-EDS spectrum of regenerated catalyst (c).

Table S1: Comparison of benzylamine oxidation activity reported in this study with that of other reported catalysts.

Note: In order to compare the photocatalytic efficiency of our Ag_3PO_4 nanoparticles, the most efficient catalysts for the same reaction from recent literature were selected. Since experimental conditions are different in different studies, a strict comparison of the catalytic performance is impossible. Therefore, the important reaction parameters such as chemical composition of the catalyst, amount of catalyst, reactant amount, solvent, reaction time, reaction temperature and reaction atmosphere are described in the table. Most of the studies use an oxygenated atmosphere as oxidant to carry out this selective oxidation reaction, this requires a special reaction set-up, flowing of oxygen in the reaction medium of a sealed vessel. Also seen in the table are a few studies where air is used instead of oxygen. However in the air-reactions, despite using a larger amount of catalyst and lower reactant quantity, the reactions were quite slow. In this context, we use only atmospheric air as oxidant without purging any external source of oxygen in this work. In addition, high reaction temperature has also been shown to improve the yield. Entries 7-11 in the table demonstrate the requirement of high reaction temperature for this conversion, while in this study, we carried out reaction at room temperature. In summary, even though an exact comparison is not possible, one can clearly see from the following table that even using ambient reaction conditions, the performance of the Ag_3PO_4 nanoparticles are quite higher than the other state-of-the-art catalysts.

Sr. No.	Catalyst	Catalyst Amount	Amt.of BA (mmol)	Time	Temp. (◦C)	O_2/air	Solvent	Conv. (%)	Select. (%)	Ref.
1.	**Ag_3PO_4**	**25 mg**	**1**	**40 min**	**r.t.**	**air**	**AcN**	**95**	**>99**	**Our work**
2.	$BiVO_4$/g-C_3N_4	20 mg	0.35	16 h	r.t	O_2	AcN	87.3	100	[2]
3.	Truxene conjugated polymer	10 mg	0.5	4 h	35	O_2	AcN	>99	91	[3]
4.	CdS nanosheets	8 mg	0.1	4.5 h	r.t	O_2	DMF	99	>99	[4]
5.	$CuWO_4$	20 mg	0.5	180 h	r.t.	O_2	AcN	93	99	[5]
6.	WS_2 nanosheets	-	0.1	30 h	50	O_2	AcN	90	95	[6]
7.	Au/CeO_2	-	0.2	6 h	100	O_2	1,4 dioxane	96	97	[7]
8.	g-C_3N_4	50 mg	1	3.5 h	80	O_2	AcN	99	99	[8]
9.	Au/Al_2O_3	100 mg	0.20	24 h	100	O_2	toluene	92	-	[9]
10.	Fe based MOF	75 mg	4.8	24 h	100	O_2	-	67	97	[10]
11.	Au NPs/SBA-NH_2	30 mg	0.4	24 h	100	O_2	toluene	90	-	[11]
12.	[Au_{25}]/TiO_2	10 mg	0.2	1.5 h	r.t	O_2	AcN	98	99	[12]
13.	TiO_2	10 mg	0.1	9 h	-	O_2	H_2O	81	63	[13]
14.	LDH	20 mg	0.2	5 h	-	air	AcN	100	97	[14]
15.	Cu/graphene	100 mg	1	6 h	40	O_2	Ethanol	99	93	[15]
16.	BiOBr	100 mg	0.1	14 h	r.t	air	AcN	100	100	[16]
17.	HNb_3O_8	20 mg	0.25	6 h	r.t	air	AcN	95	98.9	[17]
18.	Nb_2O_5	100 mg	5	50 h	r.t	O_2	benzene	>99	97	[18]
19.	BiVO4	20 mg	0.35	16 h	-	O_2	AcN	89	89	[19]
20.	AgI/$AgVO_3$	50 mg	0.25	12 h	-	air	AcN	88.2	96	[20]

Table S2: IR radiation effect and temperature variation during benzylamine oxidation reaction using Ag_3PO_4: Since solar light also contains IR radiation and the benzyl amine oxidation may not be a purely photocatalytic process, we carried out the following experiments that suggested that reaction indeed goes through photocatalytic process and does not involve thermo-induced photocatalytic process. We constantly checked the reaction temperature during photo-oxidation reaction and found that reaction temperature was between 30-32 ^{O}C (obtained temperature variation data with time shown in table S2 below)

Table S2: Recorded temperature of the reaction medium during the photo-oxidation reaction.

Reaction time	5 min	10 min	15 min	20 min	30 min	40 min
Temperature (^{O}C)	30	31	30	31	32	31

Note S1: Calculation of Apparent Quantum Efficiency (AQE): We calculated the AQE for photocatalytic benzylamine oxidation by carrying out the reaction under solar simulator spectra (Verasol Newport, spectrum given in Fig. S1a) with conversion of 95% within 40 min. We calculated the overall efficiency by counting the number of incident photons in full wavelength range (400-1000 nm). We have also calculated the efficiency in different wavelength region i.e. 400-500 nm, 500-600 nm, 600-700 nm and 700-800 nm by calculating number of incident photons in the respective regions. In order to calculate AQE by using natural sunlight, we carried out the reaction in direct sunlight (solar spectrum at sea level is given in Fig. S1b) with conversion of 93% within 40 min. The apparent quantum efficiency calculated by us is smaller than the actual quantum efficiency because the number of absorbed photons is always smaller than the number of incident photons.[21] The incident power on the sample is given as:

$$P_{incident} = \rho_{incident}(\lambda) \times A_{sample} \quad (1)$$

Where, A_{sample} is the area exposed to incident light (12.56 cm^2 in solar simulator and 15.89 cm^2 in direct sunlight), $\rho_{incident}(\lambda)$ is the incident power on the sample corresponding to photon of wavelength λ.

The incident powers on the sample by using solar simulator was estimated to be 732, 135, 151, 142 and 117 mW in the wavelength range of 400-1000 nm, 400-500 nm, 500-600 nm, 600-700 and 700-800 nm respectively. By using solar spectrum, incident power on sample was estimated to be 919 mW in 400-1000 nm wavelength region. The number of incident photons per second, as a function of wavelength can be expressed as:

$$N_{ph}(\lambda) = \frac{\rho_{incident}(\lambda)}{E_{ph}(\lambda)} \quad (2)$$

Where $E_{ph}(\lambda) = hc/\lambda$ is the photon energy for the corresponding wavelength. For example, the total number of photons incident on the sample per second within wavelength range of 400-1000 nm can be calculated as:

$$N_{ph,incident}(400-1000) = \int_{400}^{1000} \frac{\rho_{incident}(\lambda)\times\lambda}{hc} d\lambda \quad (3)$$

The AQE can be derived from the following equation:

$$AQE = n(No.of electronorhole) \times \frac{Number\ of\ imine\ molecule\ produced}{Number\ of\ incident\ photons} \times 100\ (\%) \quad (4)$$

For benzyl amine oxidation, $n = 2$.

Therefore, AQE in the 400-1000 nm range using solar simulator:

$$AQE = 2 \times \frac{0.00095}{0.00987} \times 100(\%)$$

$$= 19.25\ \%$$

Similarly, for 400-500, 500-600, 600-700 and 700-800 nm ranges, the calculated AQE are 12, 4.16, 2.13 and 0.01% respectively (Fig. 8a in the main manuscript).

AQE in the 400-1000 nm range while using direct sunlight:

$$AQE = 2 \times \frac{0.00093}{0.01244} \times 100(\%)$$

$$= 14.9\ \%$$

The variation (slight reduction) in the quantum efficiency under natural solar light may be due to (i) a modified solar spectrum than the ideal one we have used and/or (ii) less number of high energy photons in the 400-500 nm range.

Note S2: Proposed benzylamine oxidation reaction mechanism: As we discussed in the main manuscript that both photogenerated electrons and holes are responsible for this oxidation reaction by doing control experiments using radical scavengers. Since two holes and electrons are used for this amine oxidation reaction, the corresponding elementary steps for the reaction scheme proposed in main manuscript (Scheme 1) are as follows:

i) $h\nu\text{-}1 + Ag_3PO_4 \longrightarrow Ag_3PO_4 + e^- (*) + h^+ (*)$

ii) $O_2 + (*) \longrightarrow O_2 (*)$

iii) $O_2 (*) + e^- (*) \longrightarrow O_2^{\bullet -} (*)$

iv) $Ph\text{-}CH_2\text{-}NH_2 + (*) \longrightarrow Ph\text{-}CH_2\text{-}NH_2 (*)$

v) $Ph\text{-}CH_2\text{-}NH_2 (*) + h^+ (*) + O_2^{\bullet -} (*) \longrightarrow Ph\text{-}C^{\bullet}H\text{-}NH_2 (*) + HOO^{\bullet} (*)$

vi) $h\nu\text{-}2 + Ag_3PO_4 \longrightarrow Ag_3PO_4 + e^- (*) + h^+ (*)$

vii) $Ph\text{-}C^{\bullet}H\text{-}NH_2 (*) + HOO^{\bullet} (*) + h^+ (*) \longrightarrow Ph\text{-}C^+H\text{-}N^{\bullet}H (*) + H_2O_2 (*)$

viii) $Ph\text{-}C^+H\text{-}N^{\bullet}H (*) + e^- (*) \longrightarrow Ph\text{-}CH{=}NH (*)$

ix) $Ph\text{-}CH{=}NH (*) + Ph\text{-}CH_2\text{-}NH_2 (*) + H_2O_2 (*) \longrightarrow Ph\text{-}CH{=}N\text{-}CH_2\text{-}Ph + NH_3$

Figure S6: The different amine oxidation products obtained during this study and the corresponding NMR spectra:

(a) N-benzylidene-1-phenylmethanamine

^{1}H NMR (400 MHz, $CDCl_3$): δ_H 8.43 (s,1H), 7.82-7.80 (m,2H), 7.45-7.28 (m,8H), 4.86 (s,2H)

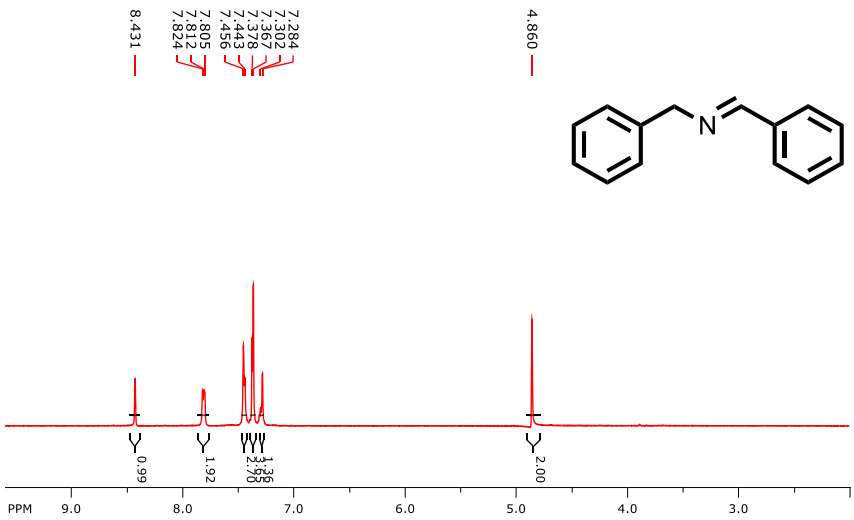

(b) N-benzylidene-1-phenylmethanamine

^{13}C NMR (400 MHz, $CDCl_3$): δ_C 162.0, 139.2, 136.1, 130.8, 128.6, 128.5, 128.2, 128.0, 127.0, 65.0.

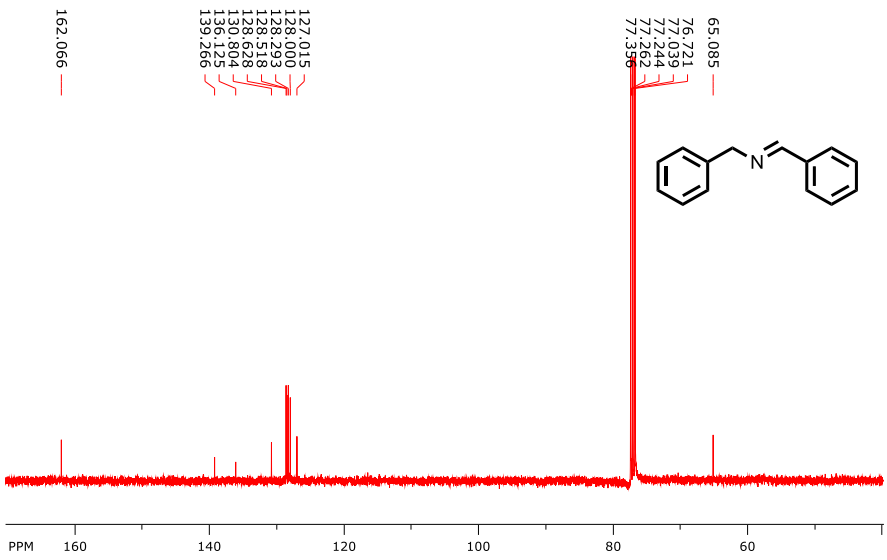

(c) N-(4-trifluoromethyl)benzylidene)-1-(4(trifluoromethyl)phenyl)methanamine

^{1}H NMR (400 MHz, $CDCl_3$): δ_H 8.49 (s,1H), 7.93 (d,2H), 7.72-7.63 (m,4H), 7.50 (d,2H), 4.92(s,2H)

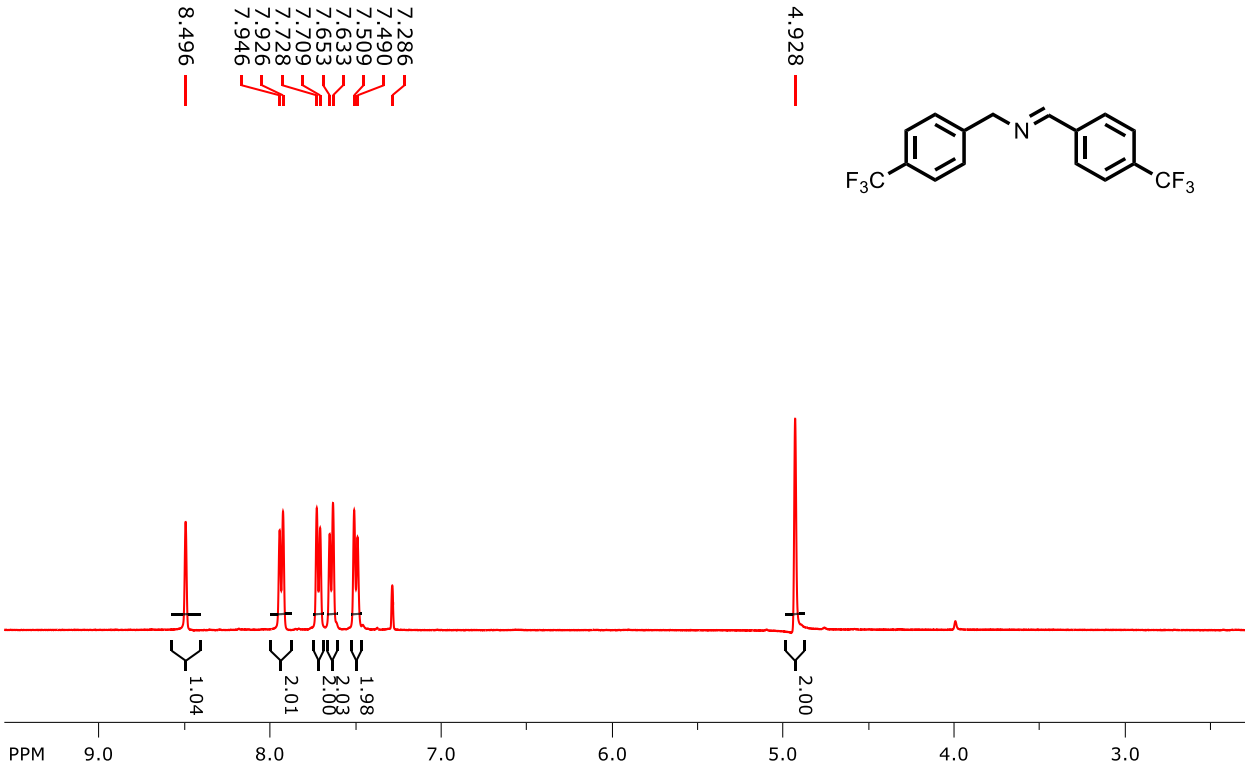

(d) N-(4-fluorobenzylidene)-1-(4-fluorophenyl)methanamine

^{1}H NMR (400 MHz, $CDCl_3$): δ_H 8.37 (s,1H), 7.81-7.78 (m,2H), 7.33-7.30 (m,2H), 7.15- 7.03 (m,4H), 4.79 (s,2H)

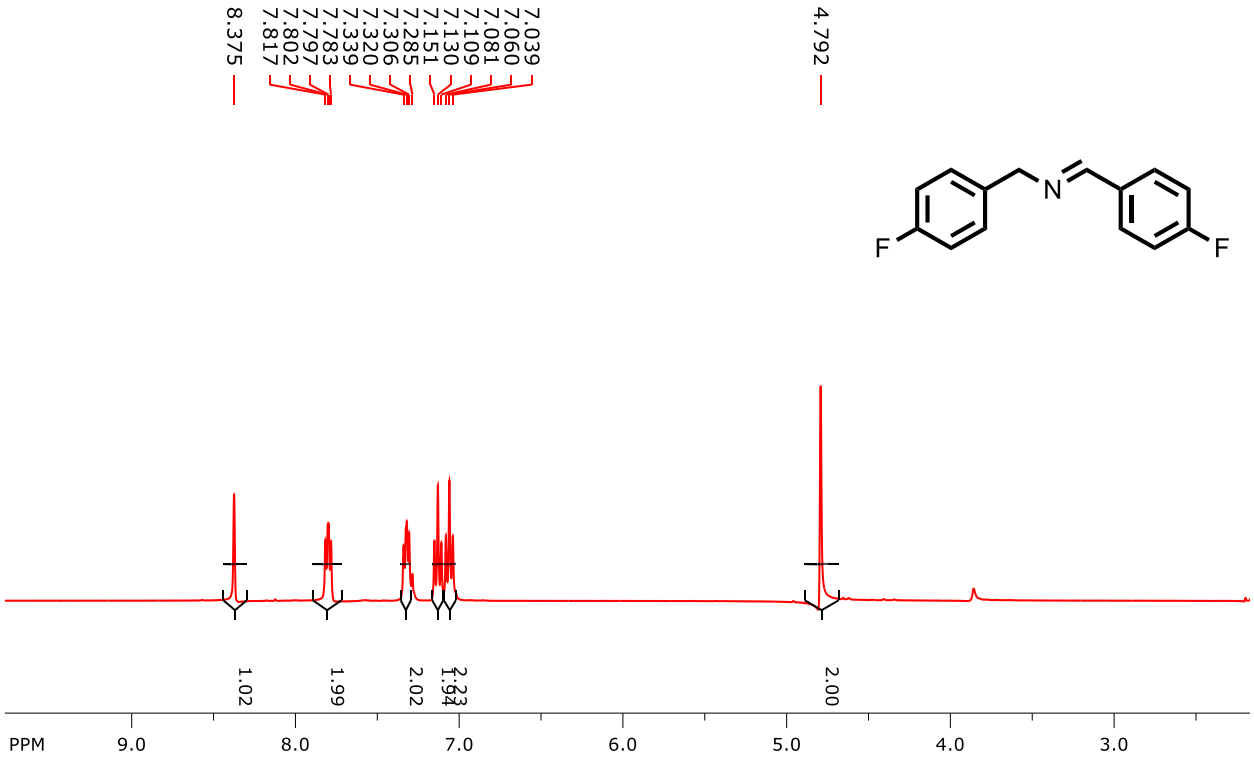

(e) N-(4-chlorobenzylidene)-1-(4-chlorophenyl)methanamine

^{1}H NMR (400 MHz, $CDCl_3$): δ_H 8.36 (s,1H), 7.74-7.72 (m,2H), 7.44 (d,2H), 7.30- 7.27 (m,4H), 4.79 (s,2H)

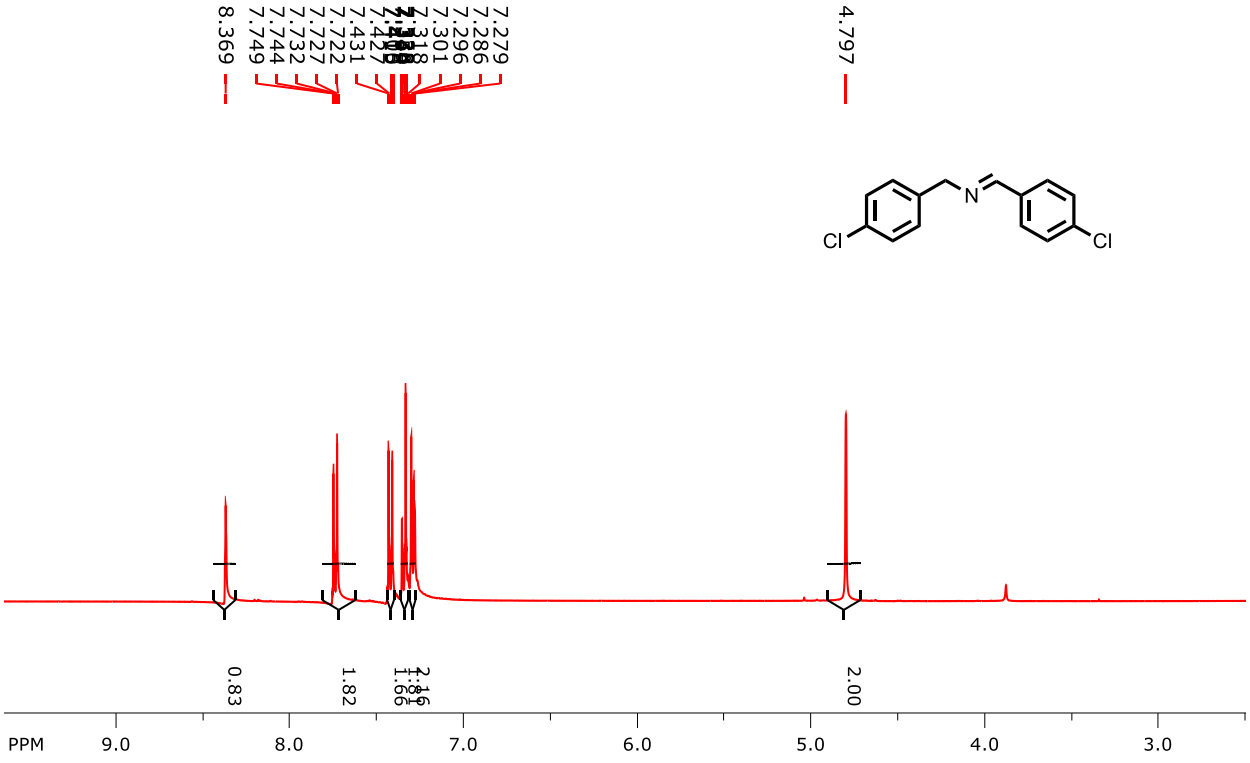

(f) N-(4-methylbenzylidene)-1-(p-tolyl)methanamine

^{1}H NMR (400 MHz, $CDCl_3$): δ_H 8.36 (s,1H), 7.69 (d,2H), 7.25-7.16 (m,6H), 4.79(s,2H), 2.40 (s,3H), 2.36 (s,3H)

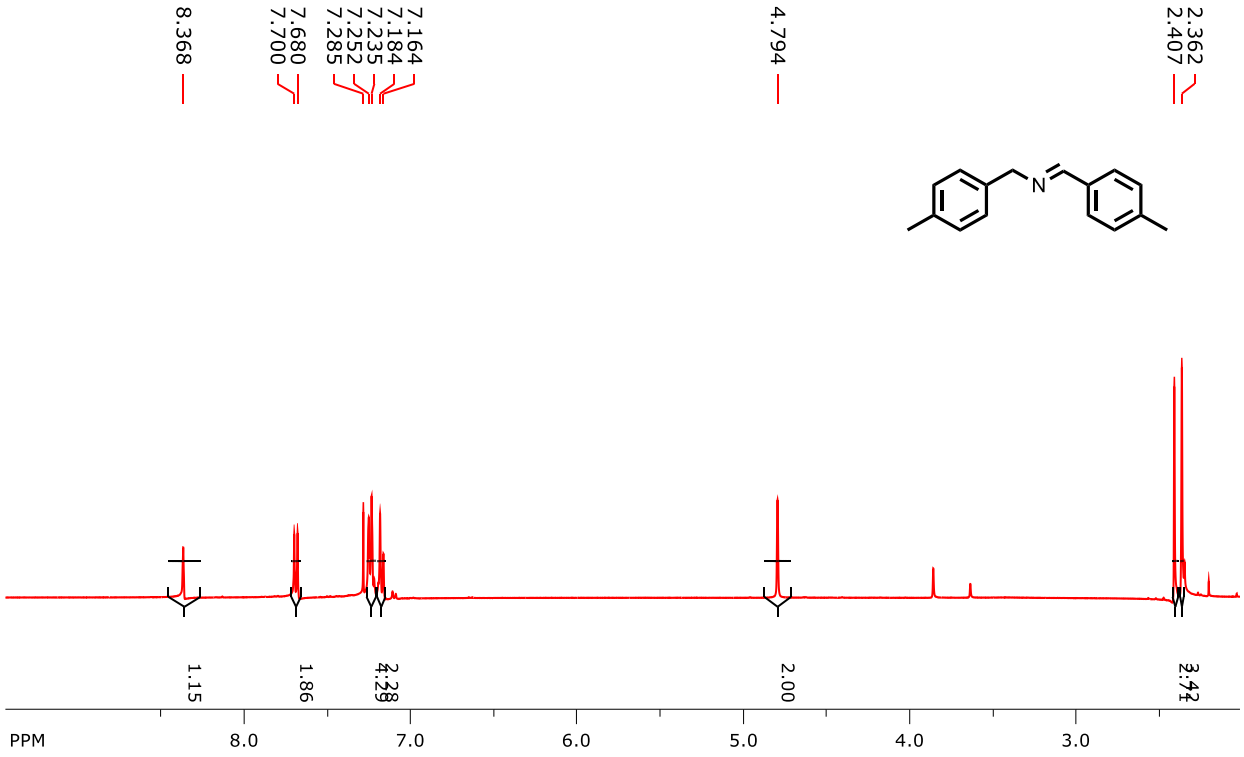

(g) N-(4-tert-butyl)benzylidene)-p-(tert-butyl)benzylamine

^{1}H NMR (400MHz, $CDCl_3$): δ_H 8.41 (s,1H), 7.77-7.75 (m,2H), 7.48-7.26 (m,6H), 4.82(s,2H), 3.87 (s, 2H), 1.36-1.31 (s, 17H)

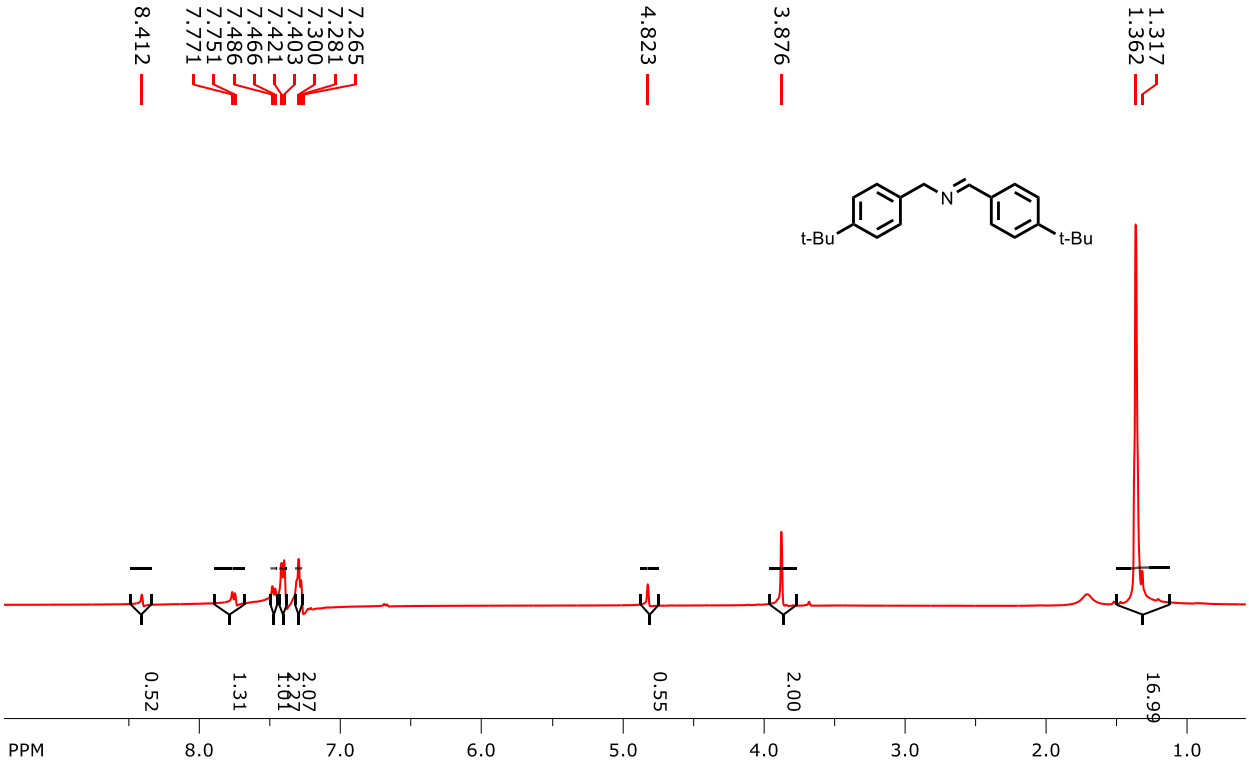

REFERENCES

(1) Marjasvaara, A.; Torvinen, M.; Vainiotalo, P. Laccase-Catalyzed Mediated Oxidation of Benzyl Alcohol: The Role of TEMPO and Formation of Products Including Benzonitrile Studied by Nanoelectrospray Ionization Fourier Transform Ion Cyclotron Resonance Mass Spectrometry. *J. Mass Spectrom.* **2004**, *39*, 1139–1146.

(2) Samanta, S.; Khilari, S.; Pradhan, D.; Srivastava, R. An Efficient, Visible Light Driven, Selective

Oxidation of Aromatic Alcohols and Amines with O_2 Using $BiVO_4$/g-C_3N_4 Nanocomposite: A Systematic and Comprehensive Study toward the Development of a Photocatalytic Process. *ACS Sustain. Chem. Eng.* **2017**, *5*, 2562–2577.

(3) Battula, V. R.; Singh, H.; Kumar, S.; Bala, I.; Pal, S. K.; Kailasam, K. Natural Sunlight Driven Oxidative Homocoupling of Amines by a Truxene-Based Conjugated Microporous Polymer. *ACS Catal.* **2018**, *8*, 6751–6759.

(4) Zhao, W.; Liu, C.; Cao, L.; Yin, X.; Xu, H.; Zhang, B. Porous Single-Crystalline CdS Nanosheets as Efficient Visible Light Catalysts for Aerobic Oxidative Coupling of Amines to Imines. *RSC Adv.* **2013**, *3*, 22944–22948.

(5) Proctor, A. D.; Panuganti, S.; Bartlett, B. M. $CuWO_4$ as a Photocatalyst for Room Temperature Aerobic Benzylamine Oxidation. *Chem. Commun.* **2018**, *54*, 1101–1104.

(6) Raza, F.; Park, J. H.; Lee, H.-R.; Kim, H.-I.; Jeon, S.-J.; Kim, J.-H. Visible-Light-Driven Oxidative Coupling Reactions of Amines by Photoactive WS_2 Nanosheets. *ACS Catal.* **2016**, *6*, 2754–2759.

(7) Wang, M.; Wang, F.; Ma, J.; Li, M.; Zhang, Z.; Wang, Y.; Zhang, X.; Xu, J. Investigations on the Crystal Plane Effect of Ceria on Gold Catalysis in the Oxidative Dehydrogenation of Alcohols and Amines in the Liquid Phase. *Chem. Commun.* **2014**, *50*, 292–294.

(8) Su, F.; Mathew, S. C.; Möhlmann, L.; Antonietti, M.; Wang, X.; Blechert, S. Aerobic Oxidative Coupling of Amines by Carbon Nitride Photocatalysis with Visible Light. *Angew. Chemie Int. Ed.* **2011**, *50*, 657–660.

(9) Zhu, B.; Lazar, M.; Trewyn, B. G.; Angelici, R. J. Aerobic Oxidation of Amines to Imines Catalyzed by Bulk Gold Powder and by Alumina-Supported Gold. *J. Catal.* **2008**, *260*, 1–6.

(10) Dhakshinamoorthy, A.; Alvaro, M.; Garcia, H. Aerobic Oxidation of Benzyl Amines to Benzyl Imines Catalyzed by Metal–Organic Framework Solids. *ChemCatChem* **2010**, *2*, 1438–1443.

(11) Jawale, D. V; Gravel, E.; Villemin, E.; Shah, N.; Geertsen, V.; Namboothiri, I. N. N.; Doris, E. Co-Catalytic Oxidative Coupling of Primary Amines to Imines Using an Organic Nanotube–Gold Nanohybrid. *Chem. Commun.* **2014**, *50*, 15251–15254.

(12) Chen, H.; Liu, C.; Wang, M.; Zhang, C.; Luo, N.; Wang, Y.; Abroshan, H.; Li, G.; Wang, F. Visible Light Gold Nanocluster Photocatalyst: Selective Aerobic Oxidation of Amines to Imines. *ACS Catal.* **2017**, *7*, 3632–3638.

(13) Lang, X.; Ji, H.; Chen, C.; Ma, W.; Zhao, J. Selective Formation of Imines by Aerobic Photocatalytic Oxidation of Amines on TiO2. *Angew. Chemie Int. Ed.* **2011**, *50*, 3934–3937.

(14) Yang, X.-J.; Chen, B.; Li, X.-B.; Zheng, L.-Q.; Wu, L.-Z.; Tung, C.-H. Photocatalytic Organic Transformation by Layered Double Hydroxides: Highly Efficient and Selective Oxidation of Primary Aromatic Amines to Their Imines under Ambient Aerobic Conditions. *Chem. Commun.* **2014**, *50*, 6664–6667.

(15) Zhai, Z.-Y.; Guo, X.-N.; Jin, G.-Q.; Guo, X.-Y. Visible Light-Induced Selective Photocatalytic Aerobic Oxidation of Amines into Imines on Cu/Graphene. *Catal. Sci. Technol.* **2015**, *5*, 4202–4207.

(16) Han, A.; Zhang, H.; Chuah, G.-K.; Jaenicke, S. Influence of the Halide and Exposed Facets on the Visible-Light Photoactivity of Bismuth Oxyhalides for Selective Aerobic Oxidation of Primary Amines. *Appl. Catal. B Environ.* **2017**, *219*, 269–275.

(17) Chen, J.; Wang, H.; Zhang, Z.; Han, L.; Zhang, Y.; Gong, F.; Xie, K.; Xu, L.; Song, W.; Wu, S. Ultrathin HNb_3O_8 Nanosheets with Oxygen Vacancies for Enhanced Photocatalytic Oxidation of Amines under Visible Light Irradiation. *J. Mater. Chem. A* **2019**, *7*, 5493–5503.

(18) Furukawa, S.; Ohno, Y.; Shishido, T.; Teramura, K.; Tanaka, T. Selective Amine Oxidation Using Nb_2O_5 Photocatalyst and O_2. *ACS Catal.* **2011**, *1*, 1150–1153.

(19) Yuan, B.; Chong, R.; Zhang, B.; Li, J.; Liu, Y.; Li, C. Photocatalytic Aerobic Oxidation of Amines to Imines on $BiVO_4$ under Visible Light Irradiation. *Chem. Commun.* **2014**, *50*, 15593–15596.

(20) Wang, X.; Yang, J.; Ma, S.; Zhao, D.; Dai, J.; Zhang, D. In Situ Fabrication of $AgI/AgVO_3$ Nanoribbon Composites with Enhanced Visible Photocatalytic Activity for Redox Reactions. *Catal. Sci. Technol.* **2016**, *6*, 243–253.

(21) Kibria, M. G.; Chowdhury, F. A.; Zhao, S.; AlOtaibi, B.; Trudeau, M. L.; Guo, H.; Mi, Z. Visible Light-Driven Efficient Overall Water Splitting Using p-Type Metal-Nitride Nanowire Arrays. *Nat. Commun.* **2015**, *6*, 6797.